Published in final edited form as:
J Biomol Struct Dyn. 2014 February ; 32(2): . doi:10.1080/07391102.2012.763216.

Systematic investigation of predicted effect of nonsynonymous SNPs in human prion protein gene: A molecular modeling and molecular dynamics study

Samad Jahandideh[*] and **Degui Zhi**
Department of Biostatistics, University of Alabama at Birmingham, Birmingham, AL 35294

Abstract

Nonsynonymous mutations in the human prion protein (HuPrP) gene contribute to the conversion of $HuPrP^{C}$ to $HuPrP^{Sc}$ and amyloid formation which in turn lead to prion diseases such as familial Creutzfeldt–Jakob disease (CJD) and Gerstmann–Straussler–Scheinker disease (GSS). In order to better understand and predict the role of HuPrP mutations, we developed the following procedure: First, we consulted the HGVBase and dbSNP databases, and we reviewed literature for the retrieval of aggregation-related nsSNPs of the HuPrP gene. Next, we used three different methods-Polymorphism Phenotyping (PolyPhen), PANTHER, and Auto-Mute -to predict the effect of nsSNPs on the phenotype. We compared the predictions against experimentally reported effects of these nsSNPs to evaluate the accuracy of the three methods: PolyPhen predicted 17 out of 22 nsSNPs as “probably damaging” or “possibly damaging”; PANTHER predicted 8 out of 22 nsSNPs as “Deleterious”; Auto-Mute predicted 9 out of 20 nsSNPs as “Disease”. Finally, structural analyses of the native protein against mutated models were investigated using molecular modeling and molecular dynamics simulation methods. In addition to comparing predictor methods, our results show the applicability of our procedure for the prediction of damaging nsSNPs. Our study also elucidates the obvious relationship between predicted values of aggregation-related nsSNPs in HuPrP gene and molecular modeling, and molecular dynamics simulations results. In conclusion, this procedure would enable researchers to select outstanding candidates for extensive molecular dynamics simulations in order to decipher more details of HuPrP aggregation.

Keywords

Human Prion Protein (HuPrP); Creutzfeldt–Jakob Disease (CJD); Gerstmann–Straussler–Scheinker disease (GSS); nsSNPs; Molecular Dynamics (MD)

INTRODUCTION

HuPrP diseases are neurodegenerative disorders that may present as acquired, sporadic or genetic forms (Prusiner, 1982). These diseases involve assembling amyloid aggregates of the prion protein, which leads to the conversion of the prion protein (PrP^{C}) from its natural conformation into a pathogenic isoform (PrP^{Sc}). This conversion includes a transition of alpha helix structures into beta sheets; however, processes associated with the conversion are not clearly determined (Pan et al., 1993; Liemann & Glockshuber, 1998). Up to now,

[*]**Address for Manuscript Correspondence:** Section on Statistical Genetics Department of Biostatistics School of Public Health University of Alabama at Birmingham Fax: 001-205-975-2540 Tel: 001-205-975-9208 sjahandideh@uab.edu.
Current address: Godzik Lab, Sanford Burnham Medical Research Institute, La Jolla, CA sjahandideh@sanfordburnham.org

sequencing the HuPrP gene from samples which show phenotypic effects has shown several nsSNPs associated with HuPrP. For example, P105L, A117V, D178N, F198S, E200K, D202N, R208H, Q212P, Q217R, M232R and V210I have been reported dozens of times (Harrison et al., 1997; Watanabe et al., 2006), and most researchers have used a molecular dynamics technique to investigate the molecular-level cause of prion diseases (Woulfe et al., 2005; Ott et al., 2008). However some mutations have not been investigated theoretically to date. Therefore, a comprehensive investigation of nsSNPs of HuPrP would be welcomed.

Through the past few years, such sequence- and structural-based computational algorithms as PolyPhen, PANTHER, and Auto-Mute have been developed to screen for deleterious nsSNPs and to predict whether the functional consequences of an nsSNPs is disease-related or neutral.

In this investigation, nsSNPs of HuPrP gene were retrieved and the different computational algorithms were used to predict the phenotypic effect of nsSNPs of HuPrP. The accuracy of the methods was calculated by comparing each method's prediction with the experimentally reported phenotypic effect of the nsSNPs. In addition, the predicted values were compared with molecular modeling and molecular dynamics simulation results. Using this procedure we were able to more effectively identify the nsSNPs on the structure and function of our protein of interest. The method enables us to select outstanding candidates for comprehensive molecular dynamics simulations and thus to decipher more details of the functional effects of disease-related mutations. Figure 1 briefly shows our methodology for analysis of nsSNPs of HuPrP.

MATERIALS AND METHODS

Database of nsSNPs

For the retrieval of aggregation-related nsSNPs of HuPrP we used Human Genome Variation database, HGVBase (http://hgvbase.cgb.ki.se), and the National Center for Biotechnology Information (NCBI) database, dbSNP (http://www.ncbi.nlm.nih.gov/projects/SNP). Also we reviewed literature. Although the average number of nsSNPs per gene is highly variable, obtained results shown presence of 22 nsSNPs in this small protein which is truly a high rate.

Multiple-alignment

Multiple alignment of prion proteins from different species, was carried out using the ClustalW2 software (http://www.ebi.ac.uk/clustalw). The multiple alignment included the sequences of *Homo sapiens* (Q5U0K3); *Macaca mulatta* (Q6JL99); *Rattus norvegicus* (P13852); *Oryctolagus cuniculus* (Q95211); *Bos taurus* (A6YK35); *Sus scrofa* (P49927); *Saccaromyces cerevisiae* (Q8TFR3); *Odobenus rosmarus* (D5MDH2); *Saccharomyces cerevisiae* (E9P8P1), retrieved from the UniProt database (http://www.uniprot.org/uniprot).

Predicting effect of nsSNPs

Up to now, much web-based software has been designed to predict the effects of nsSNPs on protein function. We used three different algorithms including Polymorphism Phenotyping (PolyPhen), PANTHER, and Auto-Mute.

PolyPhen prediction is based on phylogenetic, structure, and sequence information. PolyPhen calculates position-specific independent counts (PSIC) scores for native and mutated amino acids. Then it calculates the difference between two PSIC scores and labels the results as 'benign', 'possibly damaging' or 'probably damaging'. A PSIC score difference equal and above 1.5 is predicted to be damaging (Sunyaev et al., 2000). Recently,

PolyPhen has been successfully used in screening and structural evaluation of nsSNPs of different genes (Masoodi et al., 2012; Usifo et al., 2012; Capuano et al., 2012; Gray et al., 2012; Alanazi et al., 2011).

PANTHER estimates the probability of nsSNPs causing an impact on the function of protein. It calculates the substitution position-specific evolutionary conservation (subPSEC) score based on a multiple alignment of evolutionarily related proteins (Thomasb et al., 2003). The subPSEC score is the negative logarithm of the probability ratio of the wild type and mutated amino acids at a particular position that estimates the likelihood of a functional effect from a single amino acid substitution. PANTHER subPSEC scores are values ranging from 0 (neutral) to about −10 (most likely to be deleterious). A cutoff of −3 is the previously identified cutoff point for functional significance corresponding to a 50% probability that an nsSNPs is deleterious. Some interesting applications of PANTHER for the prediction of deleterious nsSNPs in different genes have been reported (George Priya Doss et al., 2012; Hao Da, et al., 2011; Thusberg et al., 2011).

Auto-Mute uses a Random Forest-based model to predict whether amino acid substitution effects are “neutral” or “disease” (Masso & Vaisman, 2010). Training and testing of this model is based on a database including 1790 disease and neutral variations from SwissProt variant pages that can be mapped onto PDB structure. Indeed the most important limitation of Auto-Mute is need to a solved structure of native protein.

Molecular modeling

The three dimensional model of HuPrP (1hjm PDB ID) (Calzolai & Zahn, 2003) was retrieved from the Protein Data Bank (PDB) (http://www.rcsb.org/pdb). 1hjm covers 16 nsSNPs of our database. *In silico* site-directed mutagenesis was carried out on HuPrP at related positions. The 16 mutant models were built and subjected to energy minimization using the NOMAD-Ref server (http://lorentz.immstr.pasteur.fr/nomad-ref.php). Energy minimization procedures were done using the Conjugate gradients method.

Molecular Dynamics Simulation

Molecular dynamics simulations were performed using the Gromacs 4.5.4 package. The initial velocities of atoms were randomly assigned from a Maxwell distribution. A cubic box containing SPC water model was used to solvate each of mutant models of human prion protein and used periodic boundary conditions. The distance of the box edge from the molecule’s periphery was set to 0.9 nm. The systems were neutralized using Na^+ and Cl^- ions and then real minimization was performed. The entire system was heated to 300 K followed by equilibration with NVT-MD for 100 ps at a constant temperature of 300 K. After 200 ps equilibration with NPT-MD, the final structure was used to carry out 50 ns MD simulation by GROMOS96 43a1 as force field in the NPT ensemble.

Structural models analyses

In order to analyze structure of mutant models, total energy, solvent accessibility, and hydrogen bond pattern were assessed. These analyses were carried out using Sirius software (http://www.ngbw.org/sirius/), PyMOL (DeLano, 2002), Swiss-PdbViewer (Guex & Peitsch, 1997) and the NOMAD-Ref server. Analysis of the secondary structures was performed by the DSSP program (Kabsch & Sander, 1983).

RESULTS

Result of Multiple alignment

The prion proteins from variant eukaryotic species were engaged from the UniProt database and multiple sequence alignment was performed using the ClustalW2 software (Larkin et al., 2007). The results of multiple alignment demonstrated that nsSNPs are mostly located in conserved regions of HuPrP, especially if we do not consider the yeast sequence (Figure 2). On the other hand, the rate of non-synonymous mutations is unusually high in comparison with other genes. A literature review shows that, with only a limited number of exceptions, nsSNPs of HuPrP cause prion desease. For example, E219K, which is positioned in a semi-conserved region in multiple sequence alignment, has been reported as a protective mutation against sporadic CJD prion disease in Asian populations (Figure 2) (Lukic et al., 2010).

Results of nsSNPs functional effect prediction

The effects of nsSNPs were determined using the PolyPhen program. This program predicts the functional effect of nsSNPs by considering physicochemical differences and evolutionary conservation. All the 22 nsSNPs were submitted to the PolyPhen server as input. Table 1 shows the distribution of the predicted PSCI scores by PolyPhen. Predicted PSCI scores in this database ranged from 0.007 to 2.846 and %77 of nsSNPs were predicted as damaging mutations. In addition, based on the defined cut offs, %23, %36 and %41 of nsSNPs were predicted as ‘benign’, ‘possibly damaging’ and ‘probably damaging’, respectively. Also we used PANTHER to predict effect of nsSNPs on HuPrP function. Obtained results show that %36 of nsSNPs with significance level of %50 probability were predicted as deleterious nsSNPs (Table 1).

In addition to PolyPhen and PANTHER, which are sequence-based predictor methods, we also used Auto-Mute, which is a structure-based method. In order to use this method, we first we needed to a valid PDB ID of HuPrP. A search in the Protein Data Base (PDB) revealed that the whole of the HuPrP structure is not yet solved. However, we selected 1hjm PDB ID to use with Auto-Mute. This structure covers 16 out of 22 nsSNPs. Auto-Mute, in addition to predicting the functional effect of nsSNPs, also determines location (surface, undersurface, or buried) and secondary structure (helix, strand, coil, or turn) of nsSNPs.

Auto-Mute predicted %44 of nsSNPs as “neutral” and the others as “disease”. In addition, the distribution of nsSNPs in terms of location was %37.5, %44 and %18.5 for surface, buried, and undersurface, respectively (Table 1). Results show the dominance of the buried location of nsSNPs in HuPrP. Also secondary structure position of nsSNPs is presented in Table 1.

In conclusion, as shown in Table 1, outputs of three different models are mostly consistent with each other. 6 out of 20 nsSNPs were predicted deleterious by these three models. However, PolyPhen and PANTHER are sequence-based versus Auto-Mute, which is a structure-based model and requires a solved structure of native protein, which is a significant limitation of Auto-Mute model in cases where no structure is available.

Results of analysis of mutation effect on structure

Solvent accessibility of all mutated proteins versus native protein was computed with the Swiss-PdbViewer. Solvent accessibility calculations are based on molecular surface, which is defined as the area that can be reached with the surface of a solvent molecule (radius = 1.4 A). The complete results for the native protein (1jhm) after energy minimization and for mutated proteins are presented in Table 2. Because protein functionality occurs on the surface of the protein, solvent accessibility gives a useful insight. Obtained results show a

decrease of solvent accessibility area of four mutated proteins (Table 2). In addition to solvent accessibility, it can be seen from Table 2 that the total energies for four of the mutated structures are lower than the native structure. Also, among mutations only M129V and A133V show change in number and/or pattern of hydrogen bonds.

Molecular dynamics

Root mean squared deviation (RMSD) values obtained from the backbone of seventeen model structures after 50 ns MD simulations are shown in Figure 3. Investigation of the RMSD values for mutant structures and wild type human prion protein showed that RMSD values for the sixteen mutant molecules followed different degrees of variations, with a maximum RMSD value of approximately 0.9 nm for F198V. During the simulation time, the trends of RMSD followed different patterns for mutant structures; however, the average RMSD value of some structures was increasing slightly. Thus, it is not unlikely that these deviations in those mutant structures could extol conformational rearrangements.

Root mean-squared fluctuations (RMSFs) during the MD simulations of wild-type model and mutant structures are shown in Figure 4. Investigation of RMSF values shows remarkable fluctuation events around a region covering residues (130-205). The mentioned region consists of a loop, β1-strand, Helix 1, another loop, β2-strand and Helix 2 structures for all mutant structures. The highest fluctuation values are observed in the C-terminus of Helix 1 around residues (135-145) and the C-terminus of Helix 2 (residues 185-200), with a maximum value of approximately 0.6 nm and 0.8 nm, respectively. Considering that major fluctuations occur in regions far from mutation sites, it may be supposed that long-range interactions are responsible for these conformational fluctuations in mutant structures.

Maps of secondary structure changes attained from MD simulations are shown in Figure 5. According to our results, we can demonstrate that the pattern of shifts is similar in most of the mutant models. During the simulations of most of the mutant structures in the C-terminus of Helix 2, the secondary structure shifts between helix and turn structures. The secondary structure also shifts between helix and turn structures in the C-terminus of Helix 3. On the one hand, our results for mutant models H140R and V180I show that β1-strand and β2-strand extended during the simulations. On the other hand, for mutant models R208H, V210I, and E219K, β1-strand and β2-strand converted to coil structures. In summary, through a comparison of results gained from MD simulations, it can be accepted that the structure flexibility increases remarkably in Helix 1, C-terminus of Helix 2 and C-terminus of Helix 3 of these mutant structures.

In addition, the important fluctuation values occur in specific parts of the prion protein, including the residues 135-145 of Helix 1, C-terminus of Helix 2 and C-terminus of Helix 3. Therefore, we may conclude that the suggested Helix 1, C-terminus of Helix 2 and C-terminus of Helix 3 may play a role as portions of structure that tend to decrease the structural tensions by bearing the first structural shocks. We can suggest that these specific portions have a limitation threshold stimulus. The first structural fluctuations will be started in Helix 1, the C-terminus of Helix 2 and the C-terminus of Helix 3. Considering that major fluctuations occur in regions far from mutation sites, it may be suggested that long-range interactions are responsible for these conformational fluctuations in mutant structures. Also, some mutations (T183A, F198V, V210I) are located in hydrophobic core of the prion protein. Since these mutations probably play an important role in the stability of prion protein, they deeply affect the structural stability of protein in the site. Our results reveal a significant role by Helix 1, the C-terminus of Helix 2 and the C-terminus of Helix 3 in the structural stability of prion protein. Investigation of the hydrophobic core shows that some mutations lead to increased instability in portions of the structure that are normally stable, and the short β-sheet moves away from the rest of the protein (Van der Kamp & Daggett,

2010). The exposure of the hydrophobic regions, then, could increase the tendency toward aggregation.

E219K mutation

E219K, which is positioned undersurface of protein and located in Helix 3, has been reported as a protective mutation against sporadic CJD prion disease in Asian populations (Lukic et al., 2010). This mutation was predicted as “benign” by PolyPhen, PANTHER and Auto-Mute with slightly low scores in comparison with the other mutations. Structural results show that the difference of accessible surface area and total energy of this mutation in comparison with the native structure is less than the other mutations. Also, the mutated structure shows a change in hydrogen bond pattern but does not show change in the number of hydrogen bonds (Figure 6). Superimposed structure of the native protein with mutated protein E219K shown in Figure 7 highlights the change in structure of the mutated protein. From MD simulation results, the secondary structure (especially Helix 2, and Helix 3) of E219K is more stable than the native protein. However, our analysis cannot discover the mechanism of the protective effect of E219K mutated protein, and we strongly recommend extensive molecular dynamics simulations on E219K mutation in combination with damaging mutations to discover possible mechanism of protective effect.

DISCUSSION

In the present investigation, we have shown that damaging nsSNPs in HuPrP frequently occur in conserved positions. However, we have also shown that a semi-conserved nsSNP in HuPrP can be a protective mutation and can cause resistance to prion disease. Based on our results there is possibility that some of the nsSNPs are protective mutations which occur together with deleterious mutations. These nsSNPs will remain undiscovered. In order to clarifying the effect of protective mutations, we recommend further investigations on nsSNPs which occur in semi-conserved positions. In addition, we recommend designing extensive molecular dynamics studies on provided database of nsSNPs of HuPrP in order to investigate the effect of mutations on the stability of the HuPrP structure for deciphering a mechanism of prion aggregation.

In addition to comparing the different methods, by applying MD simulations we investigated the influence of several prevalent mutations which led to the formation of aggregated forms of the human prion protein even in some conserved residues located within the conserved and highly conserved sequences of HuPrP. Analysis of the results attained from our molecular dynamics simulation shows that the most fluctuations occur around residues 135-145 of the Helix 1, C-terminus of the Helix 2 and C-terminus of the Helix 3. Our analyses clearly show that a long-range effect, as a significant cause, plays the main role in these conformational fluctuations and structural conventions in mutant models of human prion protein. These point mutations may have some local impacts on the protein interactions that are requested for oligomerization into fibrillar species.

Acknowledgments

This work is partially funded by NIH Grant R00 RR024163. The authors have no conflict of interest to declare.

REFERENCE

Alanazi M, Abduljaleel Z, Khan W, Warsy AS, Elrobh M, Khan Z, Al Amri A, Bazzi MD. In silico analysis of single nucleotide polymorphism (SNPs) in human β-globin gene. PloS One. 2011; 6(10):e25876. [PubMed: 22028795]

Buchmann A, Mondadori CR, Hänggi J, Aerni A, Vrticka P, Luechinger R, Boesiger P, Hock C, Nitsch RM, de Quervain DJ, Papassotiropoulos A, Henke K. Neuropsychologia. Prion protein M129V polymorphism affects retrieval-related brain activity. 2008; 46(9):2389–402.

Calzolai L, Zahn R. Influence of pH on NMR Structure and Stability of the Human Prion Protein Globular Domain. The Journal of Biological Chemistry. 2003; 278(37):35592–96. [PubMed: 12826672]

Capuano M, Garcia-Herrero CM, Tinto N, Carluccio C, Capobianco V, Coto I, Cola A, Iafusco D, Franzese A, Zagari A, Navas MA, Sacchetti L. Glucokinase (GCK) Mutations and Their Characterization in MODY2 Children of Southern Italy. PLoS One. 2012; 7(6):e38906. [PubMed: 22761713]

Cervenáková L, Buetefisch C, Lee HS, Taller I, Stone G, Gibbs CJ Jr, Brown P, Hallett M, Goldfarb LG. Novel PRNP sequence variant associated with familial encephalopathy. American Journal of Medical Genetics. 1999; 88(6):653–56. [PubMed: 10581485]

Chen W, Van der Kamp MW, Daggett V. Diverse effects on the native β-sheet of the human prion protein due to disease-associated mutations. Biochemistry. 2010; 49(45):9874–81. [PubMed: 20949975]

DeLano, WL. The PyMOL Molecular Graphics System. DeLano Scientific; Palo Alto, CA, USA: 2002.

Doh-ura K, et al. Pro⇒Leu change at position 102 of prion protein is the most common but not the sole mutation related to Gerstmann-Straussler syndrome. Biochemical and Biophysical Research Communications. 1989; 163:974–79. [PubMed: 2783132]

George Priya Doss C, Nagasundaram N, Tanwar H. Predicting the impact of deleterious single point mutations in SMAD gene family using structural bioinformatics approach. Interdisciplinary Sciences. 2012; 4(2):103–15.

Goldfarb L, et al. Transmissible familial Creutzfeldt-Jakob disease associated with five, seven, and eight extra octapeptide coding repeats in the PRNP gene. Proceedings of the National Academy of Sciences. 1991; 88:10926–930.

Goldgaber D, et al. Mutations in familial Creutzfeldt-Jakob disease and Gerstmann-Straussler-Scheinker's syndrome. Experimental Neurology. 1989; 106:204–06. [PubMed: 2572450]

Gray VE, Kukurba KR, Kumar S. Performance of computational tools in evaluating the functional impact of laboratory-induced amino acid mutations. Bioinformatics. 2012; 28(16):2093–6. [PubMed: 22685075]

Guex N, Peitsch MC. SWISS-MODEL and the Swiss-PdbViewer: An environment for comparative protein modeling. Electrophoresis. 1997; 18:2714–23. [PubMed: 9504803]

Hao da C, Feng Y, Xiao R, Xiao PG. Non-neutral nonsynonymous single nucleotide polymorphisms in human ABC transporters: the first comparison of six prediction methods. Pharmacological Reports. 2011; 63(4):924–34. [PubMed: 22001980]

Harrison PM, Bamborough P, Daggett V, Prusiner SB, Cohen FE. The prion folding problem. Current Opinion in Structural Biology. 1997; 17:53–9. [PubMed: 9032055]

Hsiao K, et al. Mutant prion proteins in Gerstamnn-Straussler-Scheinker disease with neurofibrillary tangles. Nature Genetics. 1992; 1:68–71. [PubMed: 1363810]

Kabsch W, Sander C. Dictionary of protein secondary structure: pattern recognition of hydrogen-bonded and geometrical features. Biopolymers. 1983; 22(12):2577–637. [PubMed: 6667333]

Kitamoto T, et al. Novel missense variants of prion protein in Creutzfeldt-Jakob disease or Gerstamnn-Straussler syndrome. Biochemical and Biophysical Research Communications. 1993; 191:709–714. [PubMed: 8461023]

Larkin MA, Blackshields G, Brown NP, Chenna R, McGettigan PA, McWilliam H, Valentin F, Wallace IM, Wilm A, Lopez R, et al. ClustalW and ClustalX version 2. Bioinformatics. 2007; 23:2947–2948. [PubMed: 17846036]

Liemann S, Glockshuber R. Transmissible spongiform encephalopathies. Biochemical and Biophysical Research Communications. 1998; 250:187–193. [PubMed: 9753605]

Lukic A, Beck J, Joiner S, Fearnley J, Sturman S, Brandner S, Wadsworth JD, Collinge J, Mead S. Heterozygosity at polymorphic codon 219 in variant creutzfeldt-jakob disease. Arch Neurology. 2010; 67(8):1021–1023.

Masoodi TA, Shammari SA, Al-Muammar MN, Almubrad TM, Alhamdan AA. Screening and structural evaluation of deleterious Non-Synonymous SNPs of ePHA2 gene involved in susceptibility to cataract formation. Bioinformation. 2012; 8(12):562–7. [PubMed: 22829731]

Masso M, Vaisman II. Knowledge-based computational mutagenesis for predicting the disease potential of human non-synonymous single nucleotide polymorphisms. Journal of Theoretical Biology. 2010; 266:560–68. [PubMed: 20655929]

Mastrianni J, et al. Mutation of the prion protein gene at codon 208 in familial Creutzfeldt-Jakob disease. Neurology. 1996; 47:1305–1312. [PubMed: 8909447]

Nitrini R, et al. Familial spongiform encephalopathy associated with a novel prion protein gene mutation. Annals of Neurology. 1997; 42:138–46. [PubMed: 9266722]

Ott D, Taraborrelli C, Aguzzi A. Novel dominant-negative prion protein mutants dentified from randomized library. Protein Engineering Design & Selection. 2008; 21(10):623–29.

Pan KM, et al. Conversion of alpha-helices into beta-sheets features in the formation of the scrapie prion proteins. Proceedings of the National Academy of Sciences. 1993; 90(23):10962–66.

Panegyres PK, Toufexis K, Kakulas BA, Cernevakova L, Brown P, Ghetti B, Piccardo P, Dlouhy SR. A new PRNP mutation (G131V) associated with Gerstmann-Sträussler-Scheinker disease. Archive of Neurology. 2001; 58(11):1899–902.

Pocchiari M, et al. A new point mutation of the prion protein gene in Creutzfeldt-Jakob disease. Annals of Neurology. 1993; 34:802–07. [PubMed: 7902693]

Polymenidou M, Prokop S, Jung HH, Hewer E, Peretz D, Moos R, Tolnay M, Aguzzi A. Atypical prion protein conformation in familial prion disease with PRNP P105T mutation. Brain Pathology. 2011; 21(2):209–14. [PubMed: 20875062]

Prusiner SB. Novel protein acetous infectious particles cause scrapie. Science. 1982; 216:136–44. [PubMed: 6801762]

Sunyaev S, Ramensky V, Bork P. Towards a structural basis of human non-synonymous single nucleotide polymorphisms. Trends in Genetics. 2000; 16:198–200. [PubMed: 10782110]

Thomas PD, Campbell MJ, Kejariwal A, Mi H, Karlak B, Daverman R, Diemer K, Muruganujan A, Narechania A. PANTHER: a library of protein families and subfamilies indexed by function. Genome Research. 2003; 13(9):2129–41. [PubMed: 12952881]

Thusberg J, Olatubosun A, Vihinen M. Performance of mutation pathogenicity prediction methods on missense variants. Human Mutation. 2011; 32(4):358–68. [PubMed: 21412949]

Usifo E, Leigh SE, Whittall RA, Lench N, Taylor A, Yeats C, Orengo CA, Martin AC, Celli J, Humphries SE. Low-density lipoprotein receptor gene familial hypercholesterolemia variant database: update and pathological assessment. Annals of Human Genetics. 2012; 76(5):387–401. [PubMed: 22881376]

Van der Kamp MW, Daggett V. Pathogenic mutations in the hydrophobic core of the human prion protein can promote structural instability and misfolding. Journal of Molecular Biology. 2010; 404(4):732–48. [PubMed: 20932979]

Watanabe Y, Inanami O, Horiuchi M, Hiraoka W, Shimoyama Y, Inagaki F, Kuwabara M. Identification of pH-sensitive regions in the mouse prion by the cysteine-scanning spin- labeling ESR technique. Biochemical and Biophysical Research Communications. 2006; 350:549–56. [PubMed: 17022940]

Woulfe J, Kertesz A, Frohn I, Bauer S, George-Hyslop PS, Bergeron C. Gerstmann-Sträussler-Scheinker disease with the Q217R mutation mimicking frontotemporal dementia. Acta Neuropathologica. 2005; 110(3):317–19. [PubMed: 16025285]

Zheng L, Longfei J, Jing Y, Xinqing Z, Haiqing S, Haiyan L, Fen W, Xiumin D, Jianping J. PRNP mutations in a series of apparently sporadic neurodegenerative dementias in China. American Journal of Medical Genetics Part B: Neuropsychiatric Genetics. 2008; 147B(6):938–44.

Zheng L, Longfei J, Jing Y, Xinqing Z, Haiqing S, Haiyan L, Fen W, Xiumin D, Jianping J. PRNP mutations in a series of apparently sporadic neurodegenerative dementias in China. American Journal of Medical Genetics Part B: Neuropsychiatric Genetics. 2008; 147B(6):938–44.

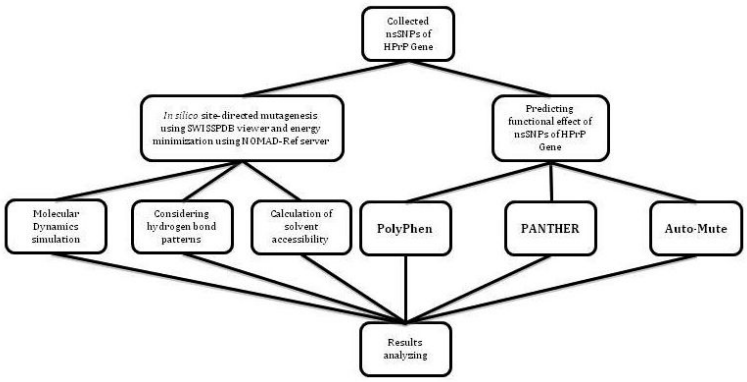

Figure 1.
Our proposed methodology for analyze of functional nsSNPs in HuPrP gene.

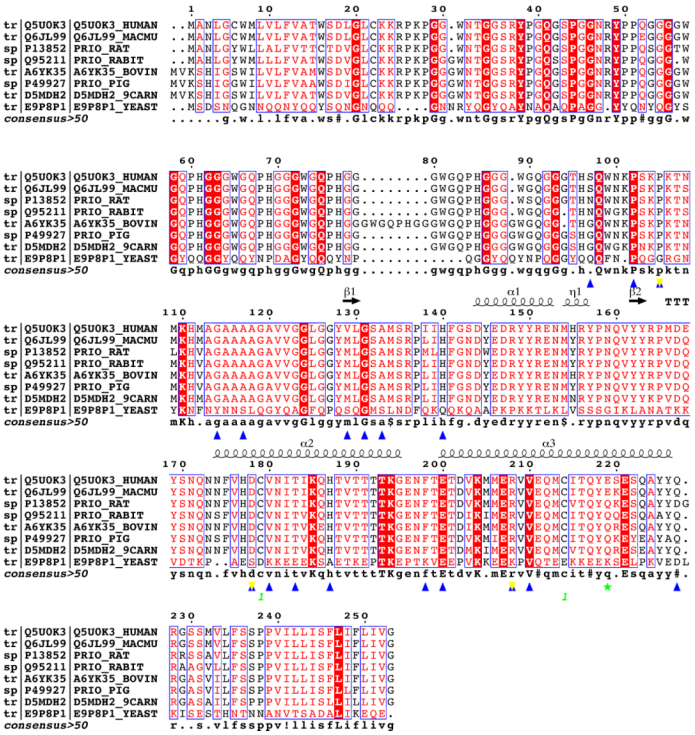

Figure 2.
Multiple sequence alignment of the prion protein from various species was done using the ClustalW2 program and annotated with ESPript 2.2. In this figure positions of 22 nsSNPs are shown. Among nsSNPs, E219K is shown with a star colored in green, which is reported as a protective mutation and cause resistance to prion disease. In addition although sequence of prion protein gene is mostly conserve, especially among mammalians, however E219K is positioned in a semi-conserved position.

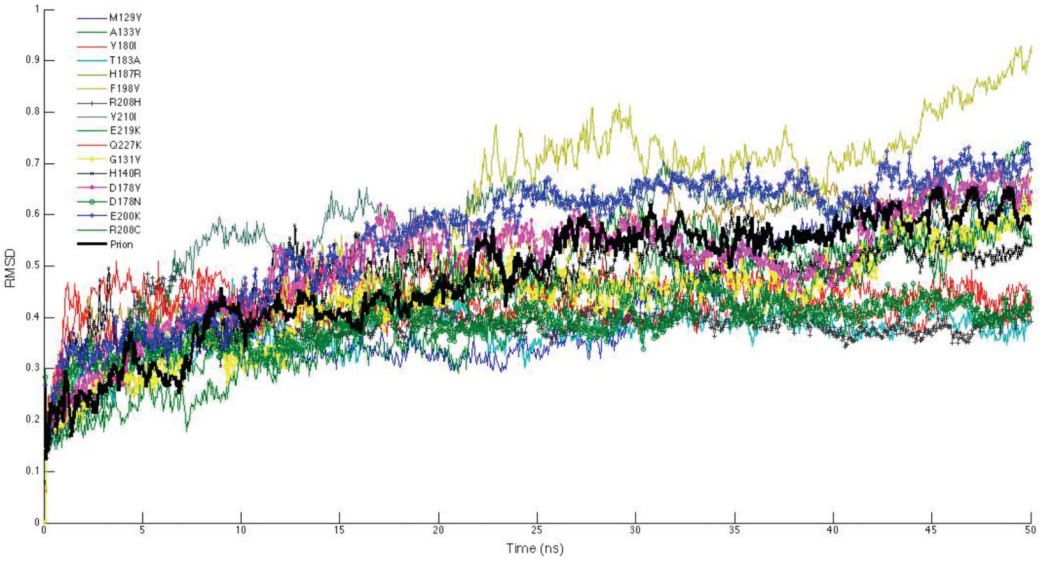

Figure 3.
Root-mean square deviations (RMSDs) of the backbone for wild-type and mutant structures. Mutations, which are likely to be damaging are shown with markers.

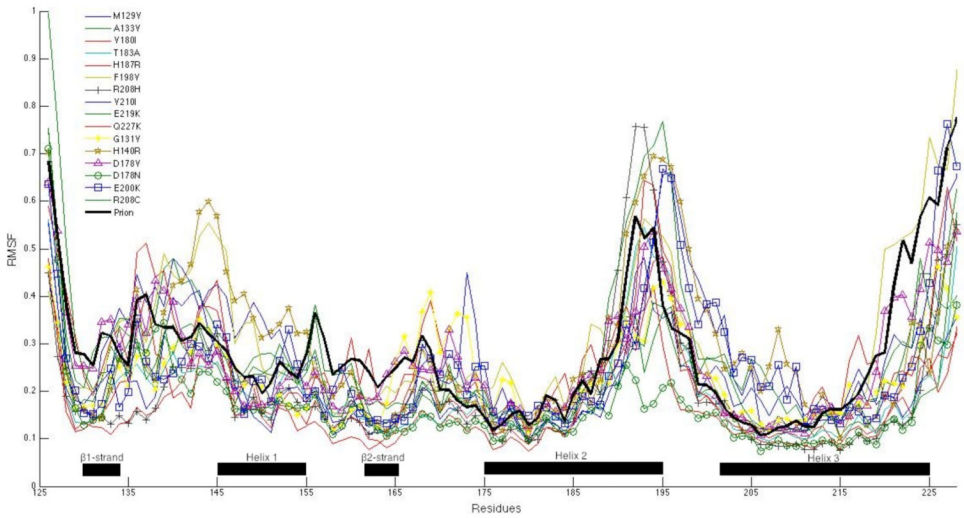

Figure 4.
Root-mean square fluctuations (RMSFs) of the alpha-carbon for wild-type and mutant structures. Mutations, which are likely to be damaging are shown with markers.

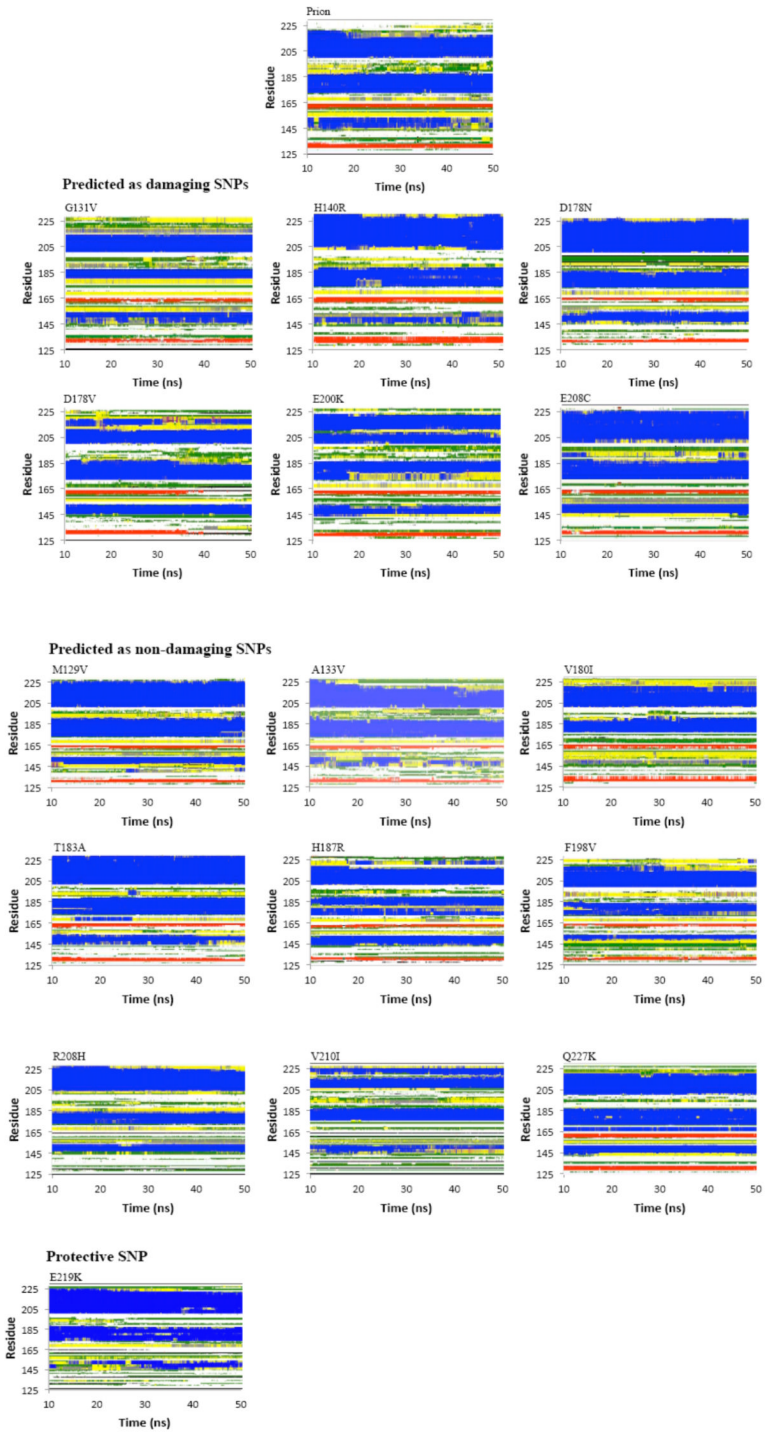

Figure 5.

Secondary structure as a function of the simulation time for wild-type and mutant structures in three different groups. Coil, B-Sheet, e-eridge, Bend, Turn, A-Helix, 5-Helix, and 3-Helix secondary structures are colored in white, red, black, green, yellow, blue, purple, and gray, respectively.

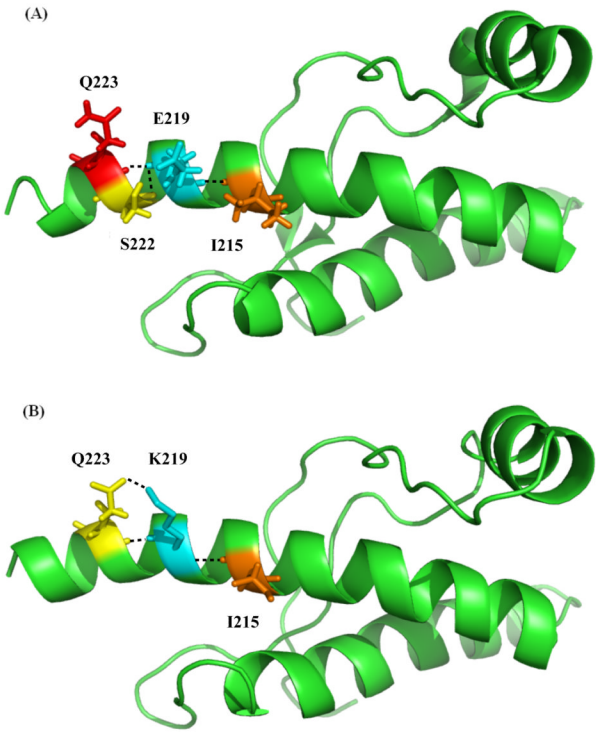

Figure 6.
Comparison of mutant models with wild type models in terms of alterations in hydrogen bond patterns. (A) showing the native type E219, (B) showing the mutant E219K. Black dotted lines are the hydrogen bonds.

Figure 7.
Superimposed structure of native protein (1hjm) with E219K mutation.

Table 1

nsSNPs that were predicted to be functionally significant by PolyPhen, PANTHER and Auto-Mute

No. of nsSNPs	nsSNP IDs	Position	Codon change	Amino acid change	Ref.	PolyPhen		PANTHER		Auto-Mute		
						PSCI score	Predicted impact	subPSEC	Pdeleterious	Predicted impact	Location of the mutated position	Secondary structure of mutated position
1	rs56362942	97	AGT ⇒ AAT	S [Ser] ⇒ N [Asn]	(Zheng et al., 2008)	0.46	Benign	−0.64168	0.08641	NA	NA	NA
2	rs74315401	102	CCG ⇒ CTG	P [Pro] ⇒ L [Leu]	(Hsiao et al., 1992)	2.846	Probably damaging	−4.19641	0.76789	NA	NA	NA
3	rs11538758	105	CCA ⇒ CTA	P [Pro] ⇒ L [Leu]	(Kiamoto et al., 1993)	2.846	Probably damaging	−3.12265	0.53062	NA	NA	NA
4	rs74315414	105	CCA ⇒ ACA	P [Pro] ⇒ T [Thr]	(Polymenidou et al., 2011)	2.396	Probably damaging	−2.40639	0.35581	NA	NA	NA
5	rs11538769	114	GGT ⇒ AGT	G [Gly] ⇒ S [Ser]	NA	1.824	Possibly damaging	−1.93207	0.2558	NA	NA	NA
6	rs74315402	117	GCA ⇒ GTA	A [Ala] ⇒ V [Val]	(Doh-ura et al., 1989)	1.542	Possibly damaging	−2.86786	0.46701	NA	NA	NA
7	rs1799990	129	ATG ⇒ GTG	M [Met] ⇒ V [Val]	(Buchmann et al., 2008)	2.234	Probably damaging	−1.41876	0.17062	Neutral	S	S
8	**rs74315410**	**131**	GGA ⇒ GTA	G [Gly] ⇒ V [Val]	(Panegyres et al., 2001)	2.499	Probably damaging	−4.26553	0.77998	Disease	U	C
9	rs74315415	133	GCC ⇒ GTC	A [Ala] ⇒ V [Val]	(Chen et al., 2010)	0.522	Benign	−1.19236	0.14092	Neutral	S	C
10	**rs11538768**	**140**	CAT ⇒ CGT	H [His] ⇒ R [Arg]	NA	2.696	Probably damaging	−3.47796	0.61727	Disease	U	C
11	**rs11538766**	**178**	GAC ⇒ GTC	D [Asp] ⇒ V [Val]	NA	2.639	Probably damaging	−4.33304	0.79134	Disease	S	H
12	**rs74315403**	**178**	GAC ⇒ AAC	D [Asp] ⇒ N [Asn]	(Goldfarb, 1991)	1.739	Possibly damaging	−3.25560	0.56355	Disease	S	H
13	rs74315408	180	GTC ⇒ ATC	V [Val] ⇒ I [Ile]	(Kiamoto et al., 1993)	0.385	Benign	−1.76721	0.22569	Neutral	B	H
14	rs74315411	183	ACA ⇒ GCA	T [Thr] ⇒ A [Ala]	(Nitrini et al., 1997)	1.825	Possibly damaging	−1.97013	0.26311	Neutral	B	H
15	rs74315413	187	CAC ⇒ CGC	H [His] ⇒ R [Arg]	(Cervenáková et al., 1999)	2.696	Probably damaging	−2.98297	0.49574	Disease	B	H
16	rs55871421	198	TTC ⇒ GTC	F [Phe] ⇒ V [Val]	(Hsiao et al., 1992)	1.933	Possibly damaging	−1.29507	0.15382	Disease	B	C
17	**rs28933385**	**200**	GAG ⇒ AAG	E [Glu] ⇒ K [Lys]	(Goldgaber et al., 1989)	1.609	Possibly damaging	−3.18946	0.54722	Disease	S	H
18	**rs55826236**	**208**	CGC ⇒ TGC	R [Arg] ⇒ C [Cys]	(Zheng et al., 2008)	2.654	Probably damaging	−4.44005	0.80846	Disease	B	H
19	rs74315412	208	CGC ⇒ CAC	R [Arg] ⇒ H [His]	(Mastrianni et al., 1996)	1.979	Possibly damaging	−2.89499	0.47377	Neutral	B	H
20	rs74315407	210	GTT ⇒ ATT	V [Val] ⇒ I [Ile]	(Pocchiari et al., 1993)	0.974	Benign	−0.63342	0.08576	Disease	B	H
21	rs1800014	219	GAG ⇒ AAG	E [Glu] ⇒ K [Lys]	NA	0.007	Benign	−0.45441	0.07272	Neutral	U	H
22	rs17852079	227	CAG ⇒ AAG	Q [Gln] ⇒ K [Lys]	NA	1.52	Possibly damaging	−0.78404	0.09833	Neutral	S	C

NA-Not Available; nsSNPs which were found to be deleterious by three models were highlighted as bold.

Table 2

Solvent accessible area and energy of the native protein and mutated proteins.

Number	Protein	Solvent accessible area Å^2	Energy (kj/mol)
1	1HJM	4912	−8033.783
2	A133V	4965	−8026.102
3	D178N	4870	−8083.750
4	D178V	4907	−7950.058
5	E200K	4971	−7995.372
6	E219K	4971	−7995.372
7	F198V	4934	−8036.745
8	G131V	4971	−7934.626
9	H140R	4937	−8308.671
10	H187R	4929	−8093.510
11	M129V	4903	−8013.048
12	Q227K	4974	−7861.952
13	R208C	4844	−7685.418
14	T183A	4961	−7991.765
15	V180I	4950	−8021.002
16	V210I	4939	−8033.883
17	R208H	4895	−7730.036